www.nature.com/onc

ORIGINAL ARTICLE

Shc is required for ErbB2-induced inhibition of apoptosis but is dispensable for cell proliferation and disruption of cell polarity

AV Lucs[1,3], WJ Muller[2] and SK Muthuswamy[1,3,4]

[1]Cold Spring Harbor Laboratory, Cold Spring Harbor, NY, USA; [2]Goodman Cancer Center, McGill University, Montreal, Quebec, Canada; [3]Department of Microbiology and Molecular Genetics, Stony Brook University, Stony Brook, NY, USA and [4]Ontario Cancer Institute, Campbell Family Institute for Breast Cancer Research, Department of Medical Biophysics, University of Toronto, Ontario, Canada

Amplification and overexpression of ErbB2 strongly correlates with aggressive breast cancers. A deeper understanding of pathways downstream of ErbB2 signaling that are required for the transformation of human mammary epithelial cells will identify novel strategies for therapeutic intervention in breast cancer. Using an inducible activation of ErbB2 autophosphorylation qsite mutants and the MCF-10A three-dimensional (3D) culture system, we investigated pathways used by ErbB2 to transform the epithelia. We report that ErbB2 induces cell proliferation and loss of 3D organization by redundant mechanisms, whereas it disrupts apical basal polarity and inhibits apoptosis using Tyr 1201 and Tyr 1226/7, respectively. Signals downstream of Tyr 1226/7 were also sufficient to confer paclitaxel resistance. The Tyr 1226/7 binds Shc, and the knockdown of Shc blocks the ability of ErbB2 to inhibit apoptosis and mediate paclitaxel resistance. Tyr 1226/7 is known to activate the Ras/Erk pathway; however, paclitaxel resistance did not correlate with the activation of Erk or Akt, suggesting the presence of a novel mechanism. Thus, our results show that targeting pathways used by ErbB2 to inhibit cell death is a better option than targeting cell proliferation pathways. Furthermore, we identify a novel function for Shc as a regulator of apoptosis and drug resistance in human mammary epithelial cells transformed by ErbB2.
Oncogene (2010) 29, 174–187; doi:10.1038/onc.2009.312; published online 12 October 2009

Introduction

ErbB2/Her2/Neu is overexpressed in 25–30% of breast cancers (Slamon et al., 1987). This overexpression correlates with a poor clinical prognosis in node-positive patients (Slamon et al., 1989). ErbB2-targeted therapies such as trastuzumab, a humanized anti-ErbB2 antibody, or Tykerb, a small molecule kinase inhibitor, are used to treat ErbB2-positive patients. The combination of anti-ErbB2 therapy with chemotherapeutic drugs, such as paclitaxel or an anthracycline/cyclophosphomide regime, shows synergistic response in controlling the disease (Slamon et al., 2001; Romond et al., 2005). However, only one-third of ErbB2-positive tumors respond to trastuzumab treatment and those that do acquire resistance within three years after the initiation of treatment (Nahta and Esteva, 2007). The quick onset of resistance and the presence of de novo resistance to anti-ErbB2 therapy significantly limit the effectiveness of currently available treatments. Thus, a deeper understanding of the signaling pathways downstream of ErbB2 that regulate transformation of epithelial cells and those that block the action of cytotoxic drugs is necessary to develop additional ways to successfully treat women with ErbB2-positive breast cancers.

Others and we have shown that the activation of ErbB2 transforms epithelial cells in culture by inducing an increase cell proliferation, disrupting apical–basal cell polarity and inhibiting apoptosis (Yu et al., 1998; Muthuswamy et al., 2001; Yarden and Sliwkowski, 2001; Henson et al., 2006). As a receptor tyrosine kinase, activation of ErbB2 results in the autophosphorylation of five tyrosine sites in its cytoplasmic tail (Akiyama et al., 1991). Four tyrosine residues, Y1144, Y1201, Y1226/7 and Y1253, are each sufficient to transform fibroblasts, which relates to their ability to activate Ras/MAPK signaling pathway (Janes et al., 1994; Dankort et al., 1997). The tyrosine at position Y1028 is a negative regulator of transformation and mutation of this site augments the transforming activity of ErbB2 (Dankort et al., 1997). Although the Y1144, Y1201, Y1226/7 and Y1253 are all redundant in their ability to transform fibroblasts, they do differ in their transformative potential in vivo as mice expressing Neu-Y1226/7 induce multifocal tumors with short latency (102 ± 22 days), whereas Neu-Y1144 induce focal tumors after a long latency (152 ± 47 days) (Dankort et al., 2001b; Marone et al., 2004). It is not clear why mutant ErbB2 receptors harboring selected tyrosine residues differ in their ability to induce mammary tumorigenesis. Furthermore, it is also not clear whether the pathways activated by autophosphorylation sites differ in their ability to

Correspondence: Dr SK Muthuswamy, Cold Spring Harbor Laboratory, One Bungtown Road, Cold Spring Harbor, NY 11724, USA.
E-mail: muthuswa@cshl.edu

disrupt apical–basal polarity or inhibit apoptosis. We rationalize that investigating the mechanisms by which ErbB2 transforms three-dimensional (3D) mammary acini will provide novel insights into signaling pathways required for ErbB2 to disrupt cell polarity and inhibit apoptosis.

Using a combination of an inducible ErbB2 activation system and a 3D culture system, we show that Y1144, Y1201, Y1226/7 and Y1253 all redundantly mediate ErbB2 signaling to promote proliferation and disrupt organization of epithelial cells within the acinus. However, only Y1201 was as efficient as wild type (wt) to disrupt apical–basal polarity, and only Y1226/7 was able to inhibit cell death during morphogenesis and in response to treatment with the chemotherapy drug, taxol/paclitaxel. Furthermore, we show that the signaling adaptor molecule, Shc, which binds to 1226/7 was required for ErbB2-induced inhibition of cell death, showing that although ErbB2 uses redundant signaling pathways to disrupt normal cell properties and induce transformation, it uses specific pathways to disrupt cell polarity and inhibit cell death.

Results

Generation of ErbB2 autophosphorylation mutants that can be activated by dimerization

To investigate the effect of inducibly activating signaling pathways downstream of each autophosphorylated tyrosine residue in human mammary epithelial cells, we generated a chimeric ErbB2 receptor that will respond to a synthetic, small molecule ligand, AP1510 (herein referred to as dimerizer), but will not respond to stimulation by epidermal growth factor (EGF) family of ligands (Muthuswamy et al., 1999). We have previously shown that the activation of this chimeric receptor phenocopies wild-type ErbB2 (wtErbB2) in its ability to transform cells and activate downstream signaling pathways (Muthuswamy et al., 1999). This approach has significant benefits over using cells stably overexpressing constitutively active ErbB2, as the process of stable selection can allow cells to adapt to constitutive ErbB2 signaling and interfere with our ability to analyse signals immediately downstream of ErbB2 activation.

For this study, we engineered the ErbB2 chimera to create mutant version in which only one of the five known autophosphorylation sites is retained as a tyrosine and the others were mutated to phenylalanine residues. In addition, we also generated an ErbB2 chimera that lacks all five autophosphorylation residues. To keep nomenclature simple, we refer to the mutants by the number that corresponds to the Tyr residue that was not mutated (Figure 1a).

To generate populations of human mammary epithelial cells that express comparable levels of the chimera (Figure 1b), MCF-10A cells were infected with retrovirus expressing the ErbB2 chimera and the cells were sorted by flow cytometry using an antibody against the p75 extracellular domain of the chimeric receptor. Three populations of cells were collected, each expressing the

chimeric receptor at different levels. The lowest level of expression was gated such that there was a 6% overlap with the nonspecific signal observed in the parental MCF-10A cells that do not express the chimeric receptors and hence do not express the p75 receptor at the cell surface. Pools 2 and 3 were collected at higher levels with ∼2.5- and 5.0-fold increase over the nonspecific signal observed in parental cells. The population of cells sorted for high levels of expression (pool 3) had constitutive activation of the receptor and did not respond to the dimerizer, making them unsuitable for these studies. Cells in pool 2 respond well to ligand stimulation by an increase in receptor tyrosine phosphorylation levels over the levels of tyrosine phosphorylation observed in the unstimulated state. To confirm that the cells have comparable levels of receptor expression, we analysed monolayer cultures by immunofluorescence analysis using anti-hemagglutinin (HA) antibodies that recognize the tagged chimeric receptor. The populations with medium levels of expression had had the chimeric receptor expressed at similar levels in every cell, suggesting that the population will respond uniformly to receptor activation. We determined that this expression level and the ability to undergo dimerizer-inducible phosphorylation was stable for 4 and 10 passages after sorting. We have limited our experiments to cells within these passages.

To determine whether the receptor chimeras undergo inducible phosphorylation, cells were stimulated and the protein lysates were analysed for changes in tyrosine phosphorylation of the chimeric receptor (Figure 1c). Consistent with the fact that the ErbB2 mutants possess only one of the five autophosphorylation sites, phosphotyrosine levels in the mutants were significantly lower than those observed for the wt receptor (compare lanes 6, 8, 10 and 12 with lane 2). Interestingly, the autophosphorylation sites differed in the extent to which they were phosphorylated in response to dimerization. Y1226/7 was phosphorylated 2.5-fold more than Y1144 and Y1201, and fivefold more than Y1253. Although it is unclear why the sites are phosphorylated differentially, it is possible that Y1226/7 is phosphorylated to a greater level because it is comprised of two tyrosines immediately adjacent to each other, that it is the major phosphorylation site in ErbB2 homodimers, or that the sites are differentially sensitive to phosphatase activity. Further analysis will be required to differentiate between these possibilities.

Autophosphorylation mutants transform fibroblasts

Previous studies have shown that each of the individual tyrosine mutants, but not a mutant lacking all the five autophosphorylated tyrosine sites, were capable of transforming Rat1 fibroblasts when expressed within the context of an activated form of ErbB2 (Dankort et al., 1997). We wanted to determine whether the autophosphorylation site mutants within the context of our inducible chimeric ErbB2 retain the ability to transform Rat1 fibroblasts in an inducible manner. The wt and mutant chimeras were transiently trans-
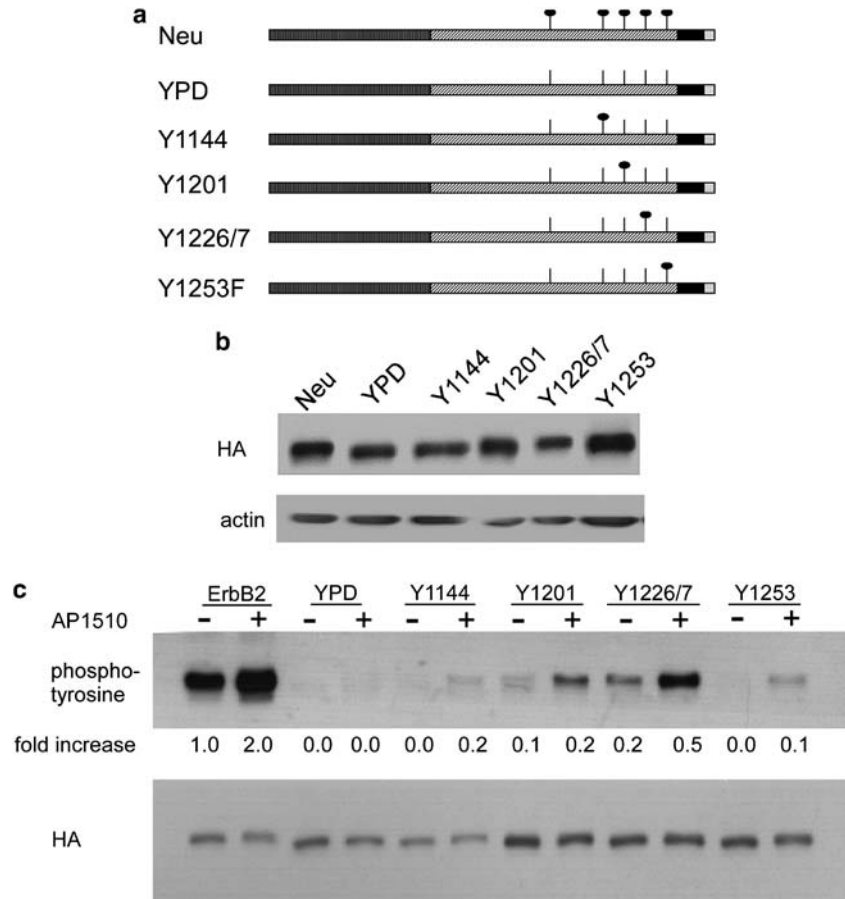
Figure 1 Inducible activation of chimeric ErbB2 and the autophosphorylation site mutants. (**a**) Schematic of a chimeric ErbB2 with the five autophosphorylated tyrosines present and a tyrosine phospho-deficient (YPD) mutant in which the autophosphorylation sites have been mutated to phenylalanine. The black and white speckled bars represent the extracellular and transmembrane domains of the low-affinity NGFR p75 receptor. The bars with black slashes represent the ErbB2 intracellular domain. The lines emanating from this domain mark the sites of the autophosphorylated tyrosines. Circles atop these lines indicate a tyrosine, their absence indicates a mutation of the tyrosine to alanine. Black bars represent the FKBP domains. The small terminal box represents the hemagglutinin (HA) tag (**b**) MCF-10As were infected with retrovirus encoding chimeric ErbB2 and the mutants. The cells were then bead selected and subsequently subjected to fluorescence-activated cell sorting to obtain comparable levels of expression. A western blot shows expression levels of pool 2, which was used for subsequent analysis. (**c**) Western blot carried out with phospho-tyrosine antibody, then stripped and reprobed for the receptor tag HA. MCF-10As expressing mutant ErbB2 were stimulated for 30 min with $1.0\,\mu\mathrm{M}$ AP1510, lysed and run out on an SDS–polyacrylamide gel electrophoresis gel. Numbers below the phosphotyrosine blot indicate the fold increase in tyrosine phosphorylation between unstimulated and stimulated samples.

fected into Rat1 fibroblasts and their foci-forming ability was assessed (Figure 2a). In the absence of receptor activation few, if any, foci were observed. Consistent with previous results, activation of wt and all of the ErbB2 mutants, with the exception of phospho-deficient mutant (YPD), induced in a significant increase in foci formation showing that they were sufficient to transform fibroblasts. Despite the differences in their phoshotyrosine content, the Y1201 and Y1253 were as potent as the wt in their ability to induce foci formation in Rat1 fibroblasts. This suggests that the stoichiometry of phosphorylation of these sites observed in the mutant receptor are similar to those observed within the context of a wt receptor. It is not clear why Y1226/7 has higher transforming ability than the wt receptor. It might be due to difference in levels of expression in Rat1 cells or due to the lack of the negative regulatory site Y1028.

Nevertheless, these data show that the inducible chimeric ErbB2 receptor phenocopies the full-length receptor in their ability to transform Rat1 fibroblast cells.

Autophosphorylation mutants transform MCF-10A 3D acini

We have previously shown that ErbB2 activation disrupts the 3D acini structures formed by MCF-10A cells grown on 3D matrix cultures. Unlike the fibroblast foci formation assay, transformation of 3D acini involves three qualitatively different events: induction of cell proliferation, disruption of cell polarity and inhibition of cell death. To investigate whether the autophosphorylated tyrosine sites differ in their ability to regulate the events required to transform MCF-10A 3D acini, we activated ErbB2 mutants in
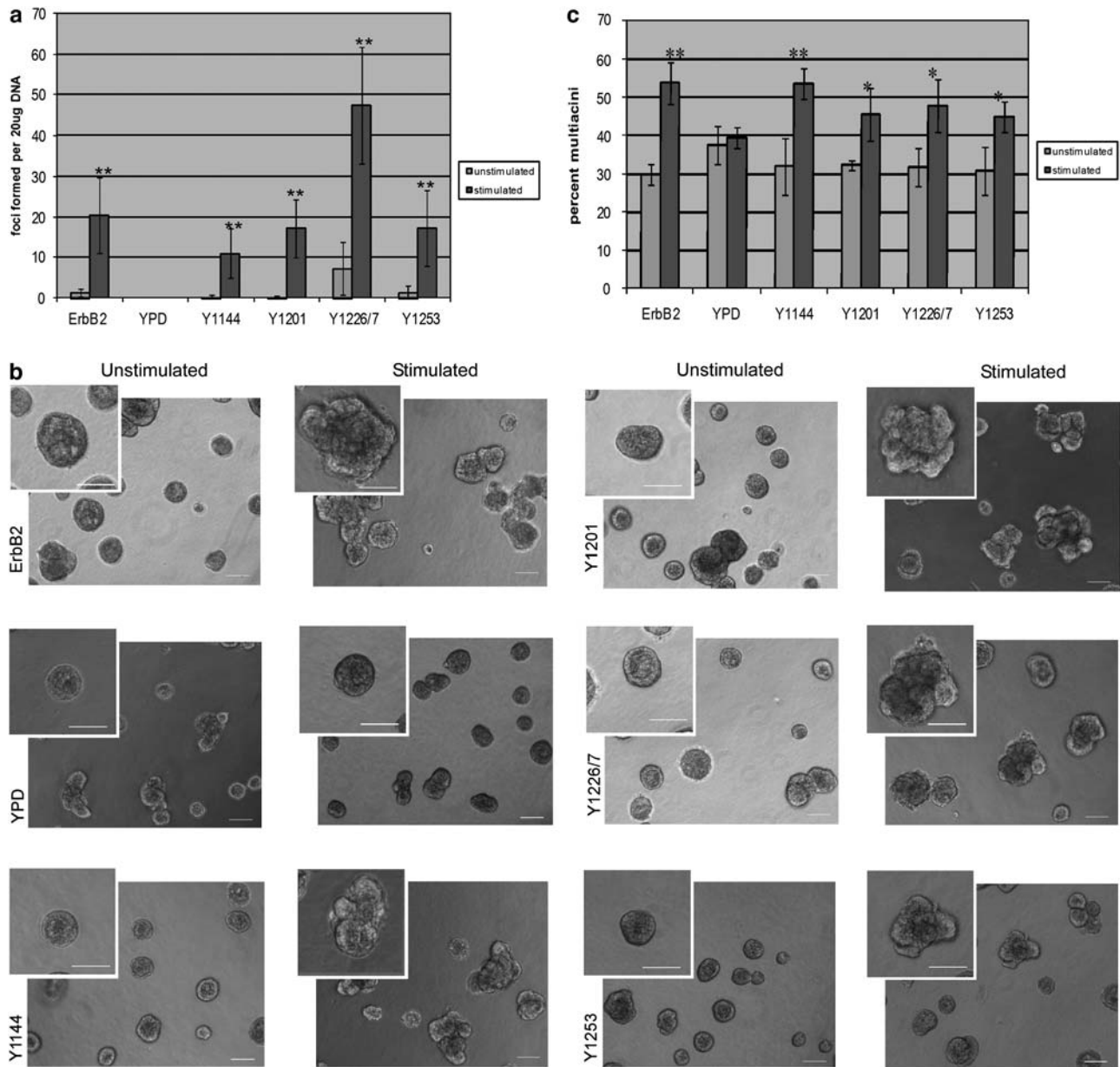
Figure 2 Autophosphorylation site mutants transform Rat1 fibroblasts and MCF-10As. (**a**) Rat1 fibroblasts were transfected on day 1 with 20 µg of DNA, stimulated with 1.0 µM AP1510 when the cells were confluent on day 3 and then grown in the presence or absence of AP1510 for the following 15 days. The plates were then fixed and stained with Giemsa and the foci were counted. Graph represents four or more experiments for each construct. (**b**) MCF-10As expressing mutant ErbB2 were plated on matrigel. Structures were grown for 12 days and then stimulated for 4 days with 1.0 µM AP1510. Phase images were taken at day 16. Scale bars represent 50 µm. (**c**) Three independent experiments were quantitated to determine the percentage of multiacinar structures in each condition. **$P < 0.005$, *$P < 0.05$.

mature, organized, 3D acini. As expected, activation of wtErbB2 induced disruption of 3D acinar organization (Figure 2b, see insert), herein referred to as a multiacinar structure. As we have reported in the past, MCF-10A cells expressing ErbB2 have a basal, dimerizer-independent, receptor phosphorylation (Figure 1c) and form multiacinar structures in 3D cultures even in the absence of small molecule ligand-induced dimerization and activation (Figure 2c). Activation of wtErbB2 resulted in 53.9% of multiacinar structures, which was 1.82-fold

higher than that observed in the absence of receptor activation. All the ErbB2 mutants, except YPD, retain the ability to induce multiacinar structures in MCF-10A 3D acini. WtErbB2 and all the mutants, except YPD, were capable of increasing rates of proliferation in the 3D structures (Supplementary Figure 1). Therefore, as observed in the fibroblast focus-forming assay, each of the four single tyrosine phosphorylation sites on ErbB2 is capable of inducing morphological disruption of MCF-10A 3D acini.

178

Tyrosine 1201 is sufficient to disrupt apical–basal polarity
ErbB2-induced disruption of acinar organization is accompanied by a disruption of cell polarity. Although disruption of cell polarity in MCF-10A 3D acini can be measured by monitoring localization of the Golgi apparatus (Aranda *et al.*, 2006), we chose to use another the epithelial cell line, Madin–Darby canine kidney II (MDCK II) cells, to directly analyse the effect of ErbB2 activation on disruption of apical–basal polarity. MDCK II cells are ideal for studying apical–basal cell polarity because the apical, lateral and apical–lateral borders can be effectively resolved using markers such as gp135 (apical), E-cadherin (lateral) and zona occludens 1 (ZO-1) (apical–lateral border). Our laboratory has previously shown that the activation of ErbB2 for 24 h results in mislocalization of tight junctions from their normal localization at the apical–lateral border in 75% of cells (Aranda *et al.*, 2006).

We generated MDCK II cells expressing the wtErbB2 or the autophosphorylation site mutants. We selected for cells expressing comparable levels of the receptor chimera. To limit variability in phenotype due to differences in expression level of the receptor, we only examined cells with a defined intensity of anti-HA signal as determined by ImageJ software (see Materials and methods section for details). In polarized MDCK cells, ZO-1 was restricted to a region of the cells that is 2.0 μm from the apical surface. Activation of ErbB2 induced mislocalization of ZO-1 to regions that are ≥ 3.0 μm below the apical membrane of the cell. Although wtErbB2 and all of the autophosphorylation site mutants were effective in disrupting cell polarity, we observed a quantitative difference in the extent to which they induced disruption of tight junctions. Activation of wtErbB2 induced mislocalization of ZO-1 in ~ 70% of cells, whereas Y1144, Y1226/7 and Y1253, but not Y1201, mutants showed significantly lower ZO-1 mislocalization (52–54%) (Figure 3). The disruption of tight junctions observed by the activation of the Y1201 mutant was not significantly different from the effect observed on activation of the wt receptor, suggesting that Y1201 was as potent as the wt receptor in its ability to disrupt apical–basal polarity.

ErbB2-induced inhibition of apoptosis is mediated by Y1226/7
We next investigated whether the ErbB2 autophosphorylation site mutants differ in their ability to inhibit cell death. Although all the mutants retained the ability to disrupt acinar structure and induce proliferation, we noticed that only the activation of Y1226/7 induced filling of luminal space in 3D acini (Supplementary Figure 2). We have previously shown that the lumen formation and maintenance in MCF-10A 3D acini is regulated by cell death (Debnath *et al.*, 2002). Thus, we investigated whether ErbB2 uses signals downstream of the Y1226/7 autophosphorylation site to inhibit apoptosis. Activation of wtErbB2 during MCF-10A morphogenesis in 3D blocks activation of caspase-3 in cells located in the luminal space (Debnath *et al.*, 2002). We

investigated whether activation of the autophosphorylation site mutants differed in their ability to inhibit activation of caspase-3. As observed for regulation of proliferation and polarity readouts, activation of YPD had no effect in the percentage of acini that stained positive for activated caspase-3. Interestingly, activation of Y1226/7 showed a significant decrease in acini with cells dying in the lumen, whereas, none of the other mutants showed significant inhibition of apoptosis (Figures 4a and b). We note that the modest decrease observed for Y1144, Y1201 and Y1253 mutants did not reach statistical significance in our experiments (see Materials and methods section for more details).

The decrease in rates of apoptosis relates to the presence of filled lumens in 3D acini. We used acini stained for 4,6-diamidino-2-phenylindole and monitored the presence or absence of cells in the lumen by optical sectioning approaches. The activation of wtErbB2 and Y1226/7 resulted in acinar structures that had lumens filled with cells, whereas acini derived from the other mutants did not show a significant increase in percentage of acini with cells in the luminal space (Supplementary Figure 2 and Figure 4c). These results show that only signals from Y1226/7 were sufficient to inhibit cell death.

Y1226/7 mediates paclitaxel resistance
Inhibition of apoptosis is particularly important in the clinic, where it contributes to resistance to cytotoxic chemotherapies.

We tested the ability of ErbB2 activation in MCF-10A cells to inhibit the death of cells treated with various cytotoxic agents. Multiple chemotherapeutic drugs blocked growth of MCF-10A cells in a dose-dependent manner (Table 1). Interestingly, short-term activation of ErbB2 did not protect cells against death induced by camptothecin, doxorubicin or etoposide (Supplementary Figure 3), whereas activation blocked cell death induced by paclitaxel (Figure 5a). Although previous studies have shown that cells overexpressing ErbB2 resist death induced by camptothecin, doxorubicin or etoposide (Knuefermann *et al.*, 2003); all those experiments were carried out using cells that were selected for high levels of expression of constitutively active ErbB2. It is likely that long-term activation of the receptor leads to activation of pathways that are not direct targets of the ErbB2 receptor, but are activated in cell populations selected for constitutive ErbB2 signaling. Our results using the inducible MCF-10A cells suggest that resistance to paclitaxel is mediated by signaling pathways directly downstream of ErbB2 activation.

To determine whether the signaling pathways downstream of the individual tyrosine sites differ in their ability to inhibit paclitaxel-induced death, we activated ErbB2 mutants with specific autophoshorylation sites. Only activation of Y1226/7 inhibited paclitaxel-induced cell death, whereas activation of YPD, Y1144, Y1201 or Y1253 was unable to inhibit paclitaxel-induced death. The inhibition of paclitaxel-induced death was observed
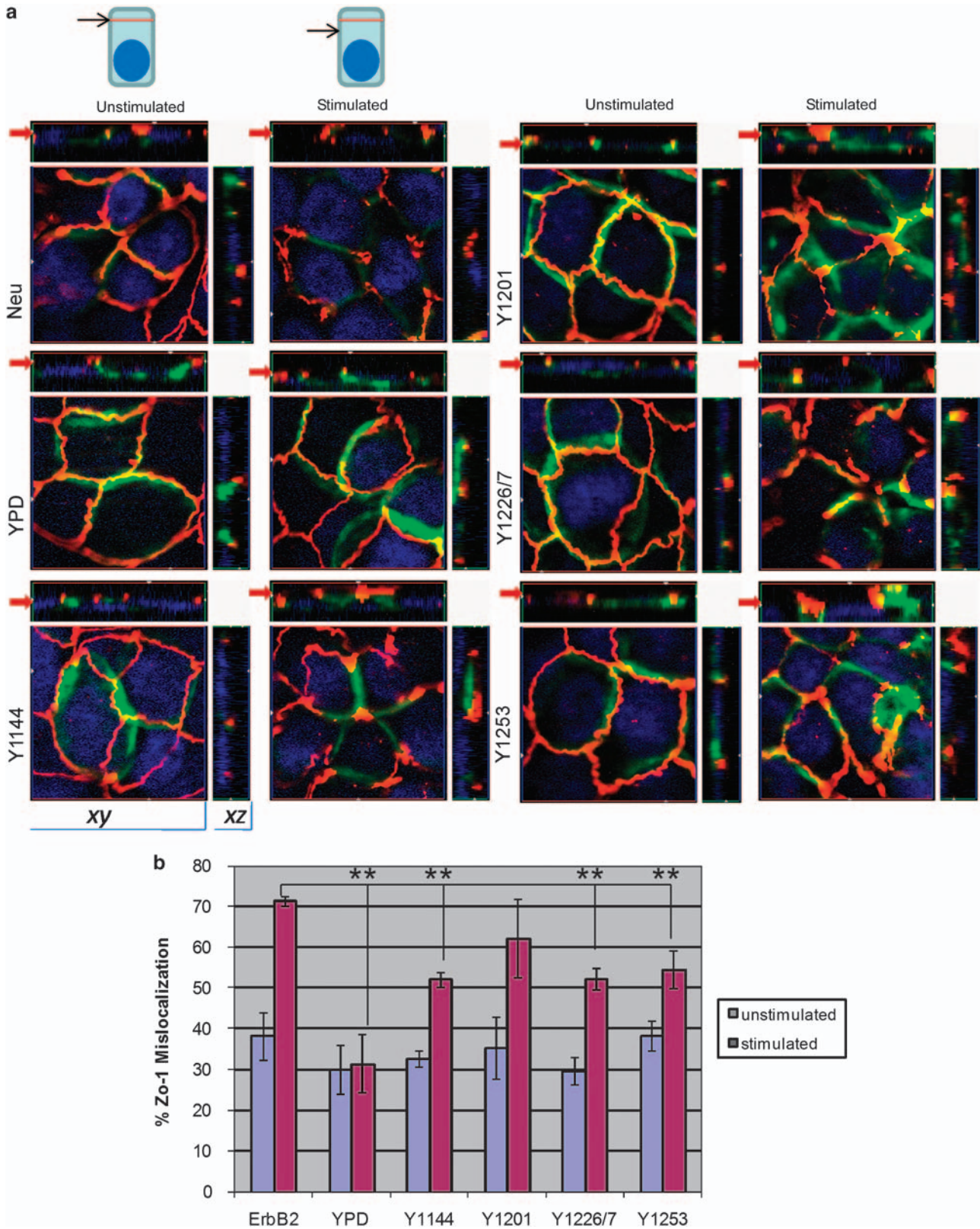
Figure 3 Y1201 disrupts apical–basal epithelial cell polarity. Madin–Darby canine kidney II cells were grown on transwell filters for 4 days and then stimulated with 1.0 μM AP1510 for 24 h. (**a**) Immunofluorescent images of the cells depict the tight junction marker zona occludens 1 (ZO-1) in red. Expression of the receptor is determined by staining the cells for the hemagglutinin (HA) tag, as visualized in green. The nuclei have been stained blue with 4,6-diamidino-2-phenylindole. Square images, xy views; top and side images, xz views. Red arrows, plane of xz view that was chosen for the xy view, also represented in the schematic depiction. (**b**) Three independent experiments were quantitated to determine the percentage of cells with mislocalized ZO-1 in each condition. **$P < 0.005$.
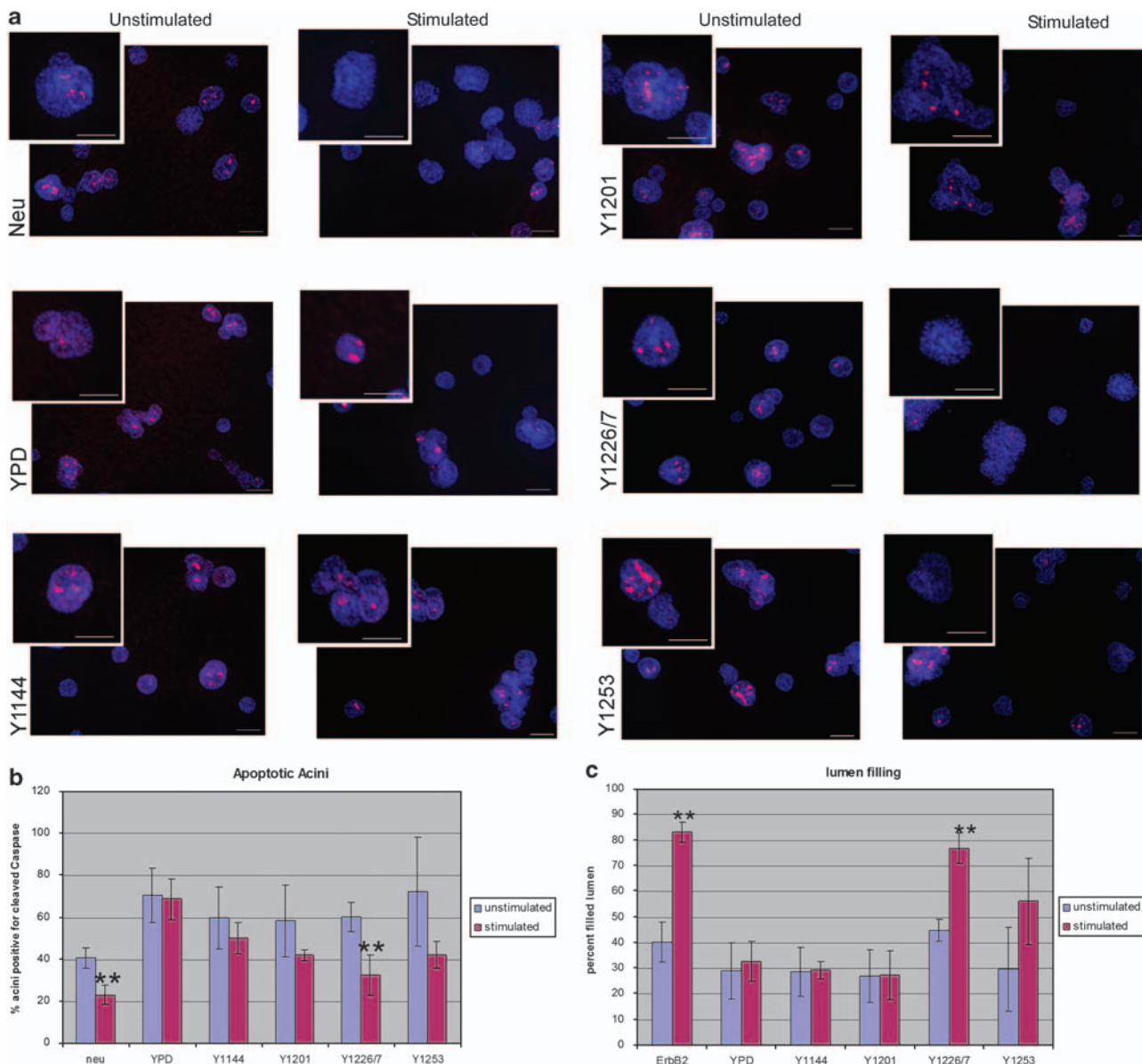
Figure 4 Y1226/7 mediates ErbB2 inhibition of apoptosis in three-dimensional (3D) epithelial structures. MCF-10As expressing mutant ErbB2 were plated on matrigel. Structures were grown for 12 days and then stimulated for 4 days with 1.0 μM AP1510, fixed and stained. Immunofluorescent images of 3D structures, in which cells express the indicated ErbB2 mutant are seen in (**a**). The apoptotic marker cleaved caspase-3 is visualized in red. The nuclei have been stained blue with 4,6-diamidino-2-phenylindole (DAPI). Scale bars represent 50 μm. (**b**) The percentage of acini positive for cleaved caspase-3 was determined in three independent experiments. (**c**) The percentage of acini with filled lumen, as determined by acini lacking DAPI staining in the center of structures, was quantitated in three independent experiments. **$P < 0.005$.

over a range of paclitaxel concentrations from 0.05 to 1.0 μM (Figure 5b and data not shown) and was comparable with the effect observed in response to activation of wtErbB2 (Figure 5b), suggesting that Y1226/7 is the principal effector of ErbB2-induced signals that inhibit apoptosis. Point mutations of ErbB2 that lack one phosphorylation site, leaving the other phosphorylation site intact, Y1226/7F or Y1253F, still retained the ability to inhibit cell death (Supplementary Figure 4), indicating that in the absence of Y1226/7, all the other sites collectively accomplish what Y1226/7 can accomplish on its own.

Y1226/7-mediated inhibition of apoptosis is independent of Erk or Akt activation
ErbB2 signaling activates two main pathways, the Ras/Erk and the PI3K/Akt pathway (Pupa *et al.*, 2005). Although the Erk pathway is thought to primarily promote proliferation, there are some indications that it can function as a cell survival signal, whereas activation of Akt pathway inhibits cell death (Wada and Penninger, 2004; Pupa *et al.*, 2005). Previous studies have shown that signaling from any of the autophosphorylation site is sufficient to activate Ras/Erk signaling (Dankort *et al.*, 2001b); consistent with this observation,

Table 1 Short-term activation of ErbB2 does not inhibit cell death induced by camptothecin, doxorubicin or etoposide

Paclitaxel (μM)	Percentage cell survival	Camptothecin (μM)	Percentage cell survival	Doxorubicin (μM)	Percentage cell survival	Etoposide (μM)	Percentage cell survival
0	100	0	100	0	100	0	100
0.01	89	0.1	93	0.05	78	10	99
0.05	62	0.5	97	0.1	63	100	37
0.1	35	1	89	0.25	71		
0.5	27	5	48	0.5	48		
1	30	10	9	1	34		

MCF-10As expressing inducible ErbB2 were plated at 0.6×10^6 cells. After 2 days the media was changed with the indicated concentrations of camptothecin, doxorubicin or etoposide in the presence or absence of $1.0\,\mu M$ AP1510. On day 4, live cells were fixed and stained with crystal violet. The amount of dye retained, which is a direct measure of live cells, was determined by lysing the cells and quantitating the dye using a spectrophotometer. The data are represented as percentage decrease in cell survival compared with the untreated control.
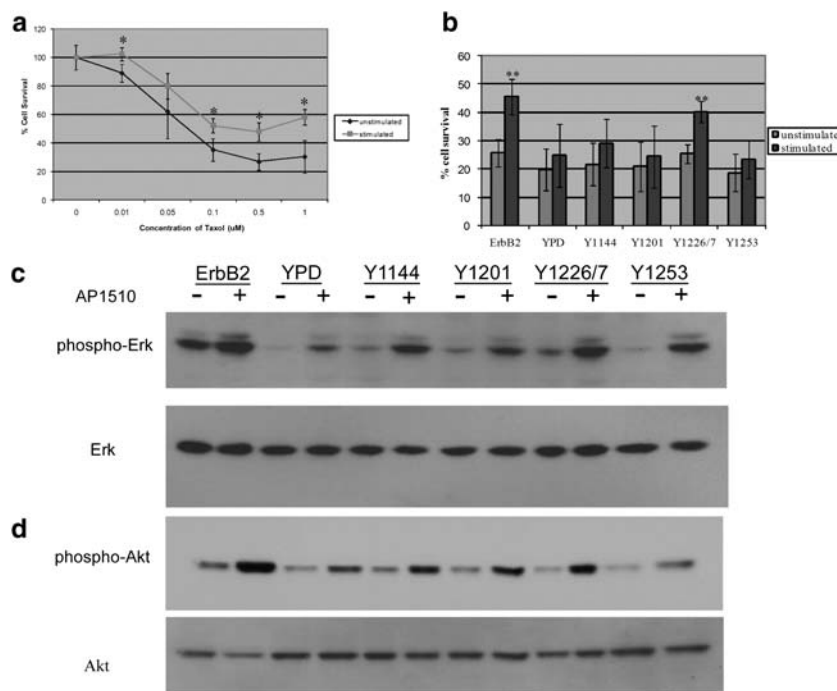

Figure 5 Y1226/7 mediates ErbB2 inhibition of paclitaxel-induced apoptosis. (**a**) Two days after plating MCF-10As, cells were treated with increasing concentrations of paclitaxel from 0.01 to $1.0\,\mu M$ in the presence or absence of $1.0\,\mu M$ AP1510. On day 4, cells were stained with crystal violet and then lysed. Relative amounts of cells survival were calculated after quantitation of the amount of crystal violet in the cell lysate, using the spectrophotometer. (**b**) A graph showing the response of cells to activation of the individual autophosphorylation site mutants in the presence of $0.5\,\mu M$ taxol ($*P<0.05$; $**P<0.005$). (**c**) MCF-10As were grown to confluency, serum starved overnight and then stimulated with $1.0\,\mu M$ AP1510 for 10 min. The membrane was first blotted for pErk and then stripped and reprobed for Erk. (**d**) Lysates were collected under the same conditions, but treated with $1.0\,\mu M$ AP1510 for 1.0 h. The membrane was first blotted for pAkt and then stripped and reprobed for Akt.

we find that activation of all ErbB2 mutants induced an increase in phosphorylation of Erk (Figure 5c). In addition, all the ErbB2 mutants were able to induce an increase in phosphorylation of Akt at ser 473, a surrogate for monitoring activation of the Akt pathway (Figure 5d). We note that the modest increase in Erk and Akt phosphorylation observed in YPD is consistent with the previous observation that YPD still retains the ability to interact with and activate c-Src tyrosine kinase (Kim *et al.*, 2005), which in turn can activate downstream signaling. Although previous studies have shown that the activation of Akt signaling regulates inhibition of cell death pathways downstream of ErbB2 and other oncogenes (Zhou *et al.*, 2000; Nelson and Fry, 2001), we did not observe any correlation between Akt activation and inhibition of paclitaxel-induced death. It is possible that the amplitude of Akt activation is not high enough for Akt to induce anti-apoptotic pathways. Consistent with this possibility, we have previously shown that ErbB2 homodimers are weaker than ErbB1/ErbB2 heterodimers of EGF ligand in their ability to activate Akt (Muthuswamy *et al.*, 1999; Zhan *et al.*, 2006).

ErbB2 induced expression of an anti-apoptotic protein, Mcl-1, which has been shown to regulate cell death (Henson et al., 2006); however, we did not observe any decrease in Mcl-1 levels in response to ErbB2 activation (Supplementary Figure 5). The redundancy with which ErbB2 activates the Erk and Akt pathways, and the lack of Mcl-1 protein regulation, suggests that Y1226/7 may facilitate activation of novel pathways to inhibit cell death in response to paclitaxel.

Shc was required for ErbB2-mediated resistance to apoptosis

Y1226/7 is known to bind the signaling adaptor Shc (Dankort et al., 2001a); however, a recent study using an in vitro Src homology 2 (SH2) and protein tyrosine-binding (PTB) domain protein array identified Syk and Abl2, in addition to Shc, as major binding partners for the Y1226/7 phosphotyrosine (Jones et al., 2006). The same study showed that Abl2 SH2 domain also interacts with Y1144 and Y1253; the Shc SH2 domain can also interact with Y1144, Y1201 and Y1253, and the Syk SH2 domain with Y1028. The Y1028 site has been identified as a negative regulatory site, which is consistent with the observations that Syk functions as a tumor suppressor in breast cancer (Coopman et al., 2000). The sequence surrounding Y1226/7 (DNLYYWDQD) conforms best to the NPXY consensus binding site for the PTB domain of Shc (Harrison, 1996). Consistent with this possibility, far-western analysis showed that the Shc-PTB domain, and not the Shc-SH2 domain, associates with Y1226/1227 (Dankort et al., 2001a). Coimmunoprecipation analysis shows that Shc does not interact with phospho Y1144, Y1201 and Y1253, whereas it interacts with Y1226/7 (Figure 5c). It is likely the data obtained from protein arrays differ from coimmunoprecipitation analysis in both stringency and sensitivity, and that Y1126/7 is the primary Shc binding site on ErbB2. Recent data identified a relationship between Shc phosphorylation and lower rates of apoptosis in polyomavirus middle T antigen-induced mammary tumors (Ursini-Siegel et al., 2008). Whether Shc has a role in ErbB2-induced inhibition of apoptosis is not known.

We hypothesized that the recruitment of Shc to the ErbB2 receptor is required for Y1226/7-induced inhibition of apoptosis. Our results show that both wtErbB2 and Y1226/7, but not the other mutants, coimmunoprecipitated with Shc, showing that activation of ErbB2 recruits Shc through Y1226/7. To rule out the possibility that Shc phosphorylation (and hence activation of a Shc pathway) can be induced by sites other than 1226/7, we analysed changes in Shc phosphorylation in response to activation of ErbB2 mutants. Both wtErbB2 and Y1226/7 induced an increase in Shc phosphorylation, whereas, other ErbB2 mutants were not capable of activating Shc (Figure 6a).

To determine whether Shc is required for Y1226/7-induced inhibition of cell death, we stably knocked down Shc expression in Y1226/7 cells using RNA interference. We generated three short hairpin RNAs that induced a 6- to 15-fold decrease in the p46 Shc protein levels, an 8- to 35-fold decrease in the p52 Shc protein levels, and a 10- to 100-fold decrease in the p66 Shc protein levels in 10A-Y1226/7 cells (Figure 6b). Y1226/7 is thought to mediate activation of the Erk pathway by recruiting Shc to the membrane (Dankort et al., 1997). Therefore, we expected that a functional Shc knockdown in these cells would decrease Erk phosphorylation in response to ErbB2–Y1226/7 activation. Y1226/7 receptor induced phosphorylation of Erk and Akt was two- to threefold weaker in Shc RNA interference cells compared with the parental cells, showing that knockdown of Shc interferes with signaling by ErbB2 (data not shown).

All three Shc knockdown cell populations were analysed for the effect of Y1226/7 activation-induced inhibition of paclitaxel-induced cell death (Figure 6c). Downregulation of Shc inhibited the ability of Y1226/7 to block cell death showing that Shc has a critical role during Y1226/7-induced inhibition of apoptosis.

To determine whether Shc is a critical effector of the anti-apoptotic signals generated by wtErbB2, we knocked down Shc in 10A-ErbB2 cells (Figure 7a) and investigated whether activation of wtErbB2-induced inhibition of apoptosis in 3D structures requires Shc. Although the activation of ErbB2 inhibited luminal apoptosis in control 3D acini, activation of ErbB2 was not able to inhibit apoptosis in cells knocked down for Shc expression (Figures 7b and c).

Thus, our results show that ErbB2 uses nonredundant mechanisms to inhibit cell death by activating an Shc-dependent signaling pathway.

Discussion

Here we use inducible ErbB2 activation system and 3D cell culture to better understand ErbB2-induced biological effects in human mammary epithelial cells. We show that ErbB2 uses redundant mechanisms to induce cell proliferation, whereas it is more selective in pathways used to disrupt cell polarity and inhibit cell death. Only activation of Y1201 was as potent as wtErbB2 in its ability to disrupt apical–basal polarity and only Y1226/7 is sufficient for the inhibition of cell death. The ability of Y1226/7 to inhibit cell death required the signaling adaptor molecule Shc. Although Shc is a known regulator of cell proliferation pathways, its role in cell death is not well understood. Thus, we have identified specific autophosphorylation residues that are sufficient to trigger cell biological effects relevant to cancer. In addition, we have defined a novel role for Shc as a regulator of cell death pathways in ErbB2-mediated transformation of mammary epithelial cells.

Consistent with previous studies, our results obtained using inducible ErbB2 autophosphorylation site mutants show that phosphorylation of Y1144, Y1201, Y1226/7 or Y1253 residues is sufficient to induce cell proliferation and activate the MAP kinase and Akt signaling pathways. These observations highlight the

robustness with which ErbB2 signals to induce cell proliferation and transform the mammary epithelia. It also raises caution about developing strategies to target pathways downstream of ErbB2 that regulates cell proliferation because it is more likely that ErbB2 will overcome the inhibition by activating alternate pathways to drive cell proliferation.

ErbB2 was selective in its ability to disrupt polarity. Only activation of Y1201 phenocopied wtErbB2; however, Y1144, Y1226/7 and Y1253 are all capable of inducing a partial disruption of polarity (Figure 3). We have recently shown that ErbB2 requires an interaction with Par6/aPKC, a polarity complex to disrupt cell polarity (Aranda *et al.*, 2006). Consistent with partial to complete disruption of polarity, we find that all the autophosphorylation sites retain the capacity to interact with Par6/aPKC (data not shown). Interestingly, ErbB2 also requires the Src kinase to disrupt polarity in MDCK cells (Kim *et al.*, 2005). Src interacts with the kinase domain of ErbB2, similar to Tyr 882 within the activation loop (Kim *et al.*, 2005). This tyrosine is intact in all of the autophosphorylation mutants used in this study and can thus explain the ability of Y1144, Y1226/7 and Y1253 mutants to disrupt polarity. However, except Y1201, activation of other tyrosine residues resulted in a partial effect, suggesting that

Y1201 has unique properties in addition to interacting with Src. Y1201 is known to recruit CrkII and Nck, the known substrates of Src kinase and regulators of the cytoskeleton (Dankort *et al.*, 1997; Dankort and Muller, 2000; Feller, 2001; Buday *et al.*, 2002), raising the possibility that, in addition to interacting with Src, recruitment of Src-specific substrate(s) to the proximity of the receptor is necessary to induce a complete disruption of polarity. Further analysis will be necessary to test this hypothesis.

Recent studies show that pathways downstream of Y1226/7 are also sufficient to induce migration (Marone *et al.*, 2004) and neovasculogenesis (Saucier *et al.*, 2004). Our results, together with these observations suggest that among the signaling pathways activated by ErbB2, those that are downstream of Y1226/7 uniquely regulate biological processes relevant to cell transformation and offer an opportunity for therapeutic intervention.

It is likely that understanding how Shc regulates cell death pathways will offer new therapeutic opportunities for controlling paclitaxel resistance. Our results suggest that the Shc-mediated inhibition of apoptosis is independent of activation of the Ras/MAPK signaling pathways because all ErbB2 autophosphorylation site mutants retain the ability to activate Ras/MAPK
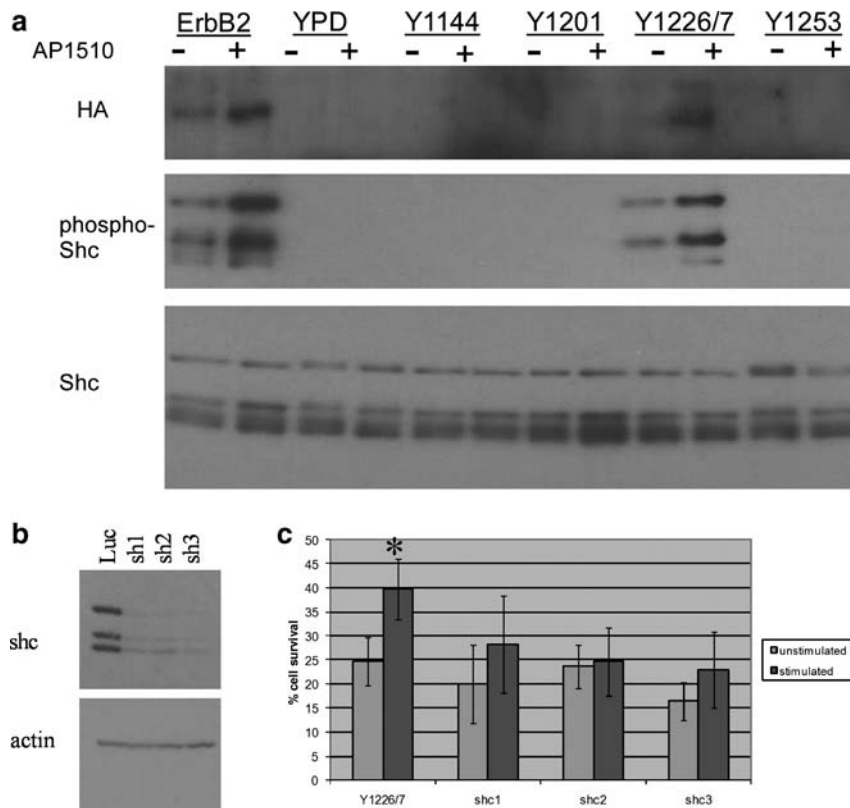

Figure 6 Y1226/7-mediated inhibition of apoptosis. (**a**) MCF-10As were grown to confluency, serum starved overnight and then stimulated with 1.0 μm AP1510 for 1.0 h. Shc was immunoprecipitated. The membrane was blotted for phospho-tyrosine and then stripped and reprobed for Shc. (**b**) Western blot showing stable Shc knockdown in MCF-10A cells using short hairpins. Expression levels were normalized to actin. (**c**) A cell survival assay as described in Figure 5 was performed using these cells. The results of three independent experiments are shown in the graph (*P < 0.05).

184
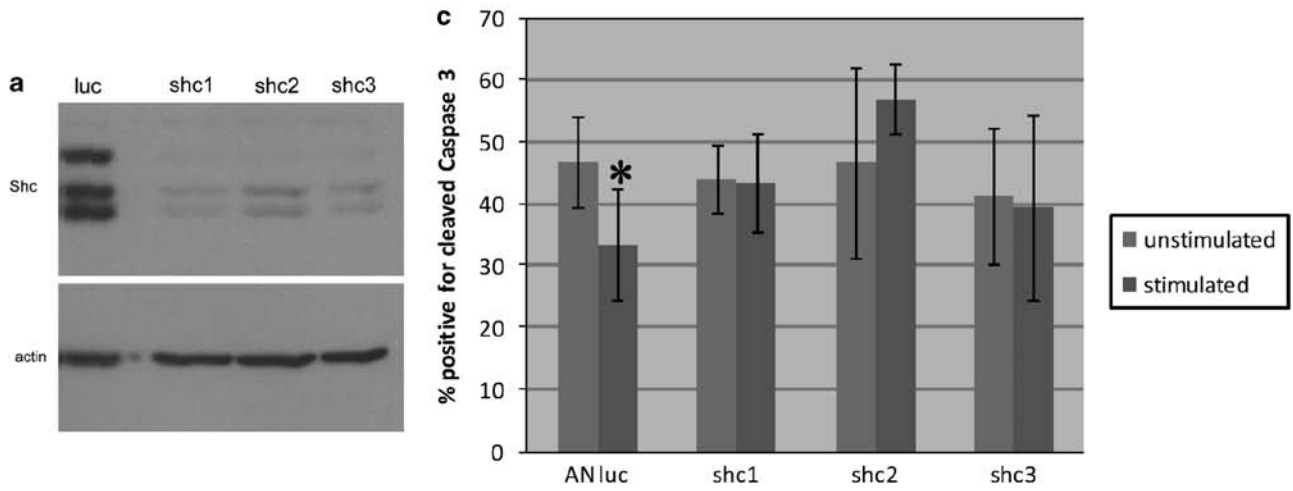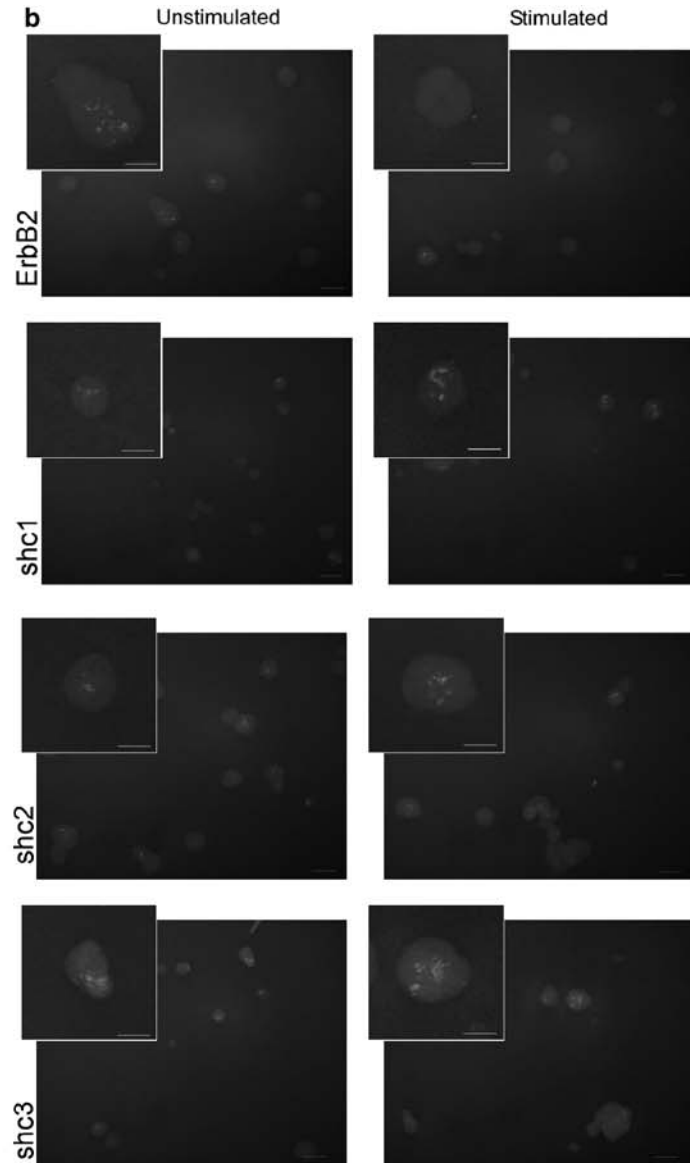
signaling (Figures 5c and d) but lack the ability to inhibit cell death (Figures 4 and 5b). Most known mechanisms of paclitaxel resistance depend on altering the dynamics of the microtubule polymerization (Orr et al., 2003). Shc can regulate microtubule dynamics by at least three independent mechanisms. Shc interacts with SHIP-2 (Habib et al., 1998), which has recently been shown to deter microtubule stabilization in mast cells (Leung and Bolland, 2007). It is possible that the Shc–SHIP-2 interaction leads to destabilization of microtubules. Shc has also been shown to interact directly with actin in PC12 cells (Thomas et al., 1995) and to cause reorganization of the cytoskeleton (Gu et al., 1999). As changes in the actin cytoskeleton can increase resistance to anti-microtubule drugs (Verrills et al., 2006), it is possible that the interaction of Shc with the actin cytoskeleton mediates resistance to taxol. Finally, the mediator of ErbB2-driven cell motility, which binds to the Y1226/7 of ErbB2, possibly through Shc, is necessary for ErbB2-induced microtubule polymerization in T47D and SkBr3 cells (Marone et al., 2004). It is also possible that Shc activates general anti-apoptotic pathways, such as upregulation of Bcl-2, Bfl-1 or downregulation of BH3 proteins, Bim, consistent with previous studies in which overexpression of Bcl-2 has been shown to inhibit apoptosis in 3D structures (Debnath et al., 2002). Interestingly, a recent study showed that the expression of a phosphorylation site mutant version of Shc (Y313F) increases cell death in a polyomavirus mT mouse model of mammary tumorigenesis, suggesting that the ability of Shc to regulate cell survival pathways is not limited to ErbB2-dependent tumors (Ursini-Siegel et al., 2008). A deeper analysis to understand how Shc signals to inhibit paclitaxel-induced cell death is likely to have broad clinical benefit.

Resistance to ErbB2-directed therapies in multiple clinical settings highlights the need to develop alternative treatment paradigms for ErbB2-positive tumors. Our results suggest that inhibiting cell death pathways, and not cell proliferation pathways, downstream of ErbB2 as a potentially effective therapeutic strategy as ErbB2 uses nonredundant mechanisms to inhibit cell death. Understanding the pathways downstream of the ErbB2–Shc interaction may not only identify novel combination drug targets but also identify biomarkers for predicting response to chemotherapies.

Materials and methods

Cloning of autophosphorylation site mutants
The individual autophosphorylated tyrosine sites were mutated one tyrosine at a time to phenylalanine using the Quickchange kit (Stratagene, La Jolla, CA, USA). The constructs were generated in Neu, the rat homolog of human ErbB2, intracellular domain with silent mutations abolishing the Xba restriction sites in a pCG backbone. After sequence verification, the ErbB2 intracellular domain was PCR amplified, purified, digested with Xba1/Spe1 and ligated to the retroviral vector pBabe.p75.F2.HA as previously described (Muthuswamy et al., 1999) at the Spe1 locus.

The primers used to generate the tyrosine to phenylalanine mutations were as follows: 5'-Y1028 GTAGACGCTGAA GAATTCCTGGTGCCCCAG, 3'-Y1028 CTGGGGCACC AGGAATTCTTCAGCGTCTAC, 5'-Y1144AGCCCCCAG CCCGAATTTGTGAACCAATCA, 3'-Y1144 TGATTGGT TCACAAATTCGGGCTGGGGGGCT, 5'-Y1201 GTGGAG AACCCTGAATTCTTAGTACCGAGA, 3'-Y1201 TCTC GGTACTAAGAATTCAGGGTTCTCCAC, 5'-Y1226/7 TT TGACAACCTCTTCTTCTGGGACCAGACC, 3'-Y1226/7 GG TCTGGTCCCAGAAGAAGAGGTTGTCAAA, 5'-Y1253 GA GAACCCTGAGTTCCTAGGCCTGGAT, 3'-Y1253 ATCC AGGCCTAGGAACTCAGGGTTCTC.

Cell culture
MCF-10A cells were maintained in Dulbecco's modified Eagle's medium (DMEM)/F12 (Gibco, Invitrogen, Carlsbad, CA, USA), 5% horse serum (Hyclone, Waltham, MA, USA), 1% penicillin/streptomycin (Gibco), 100 ng/ml cholera toxin, 10 μg/ml insulin, 500 ng/ml hydromycin (Sigma, St Louis, MO, USA) and 20 ng/ml EGF (Peprotech, Rocky Hill, NJ, USA). Assay media used for 3D studies was made of DMEM/F12, 2% horse serum, 1% penicillin/streptomycin, 100 ng/ml cholera toxin, 10 μg/ml insulin and 500 ng/ml hydromycin. MDCKs and Rat1 fibroblasts were grown in DMEM (Gibco), 10% fetal bovine serum and 1% penicillin/streptomycin.

Focus-forming assay
Rat1 fibroblasts were plated at 2×10^5 cells per 6-cm dish on day 0. On the next morning, cells were transfected with 10 μg pBabe p75.F2.ErbB2.HA and pBabe p75.F2.8A.HA using calcium phosphate. At 6 h after transfection, cells were washed twice with DMEM/0.5% fetal bovine serum and then incubated overnight in DMEM/10% fetal bovine serum. On day 2 the media was changed. By day 4 cells had become confluent and cells were stimulated by changing the media and adding 1.0 μM AP1510 (Ariad Pharmaceuticals, Cambridge, MA, USA). Media was changed every 3 days until day 16, when cells were fixed with 4% PFA and stained with Giemsa.

Fluorescence-activated cell sorting
MCF-10A cells expressing the chimeric receptor were dissociated by incubation at 37 °C with 10 mM EDTA:0.25% trypsin:phosphate-buffered saline for 30 min. The cells were then collected and washed twice in growth media. In all, 15×10^6 cells were resuspended in 3 ml of media and incubated for 30 min with the p75 NGFR antibody. Cells were washed three times with fresh media, resuspended in 1.5 ml media with 15 μl of anti-mouse 488 antibody and incubated at room temperature for 1.0 h before washing again three times in

Figure 7 Shc is necessary for ErbB2-induced inhibition of apoptosis in three-dimensional (3D) epithelial structures. (a) Western blot showing stable Shc knockdown in MCF-10A cells using short hairpins. Actin is shown as a loading control. (b) MCF-10A-ErbB2 cells were plated on matrigel. Structures were grown for 4 days and then stimulated for 4 days with 1.0 μM AP1510, fixed and stained. Immunofluorescence images of 3D structures stained with an apoptotic marker-cleaved –caspase-3 is shown. The nuclei are stained blue with 4,6-diamidino-2-phenylindole. Scale bars represent 100 and 50 μm in inset. (c) The percentage of acini positive for cleaved caspase-3 was determined for three independent experiments. *$P \leqslant 0.05$.

growth media. After the final wash cells were resuspended in 3.0 ml of growth media, filtered through a 3.5-μm mesh and run on the FACSVantage SE Cell Sorter (BD Biosciences, San Jose, CA, USA). The population of positive staining cells was divided into low, medium and high expressing groups, collected and returned to culture. Medium level expressing cells were used for further experiments.

3D assays

A total of 4000 cells were plated per well of an eight chamber slide coated with 70 μl matrigel in assay media containing 2.5% matrigel and 5 ng/ml EGF. Cells were cultured for 16 days, changing media every 4 days and stimulating with 1.0 μM AP1510 on day 12. Phase images on cells were taken every 4 days. After imaging on day 16, slides were fixed in 4% PFA, permeabilized in 0.5% Triton and incubated with the antibodies indicated for immunofluorescence.

MDCK polarity assay

Madin–Darby canine kidney II cells were plated on 12-well transwell filters at 0.5×10^6 cells per well and grown for 4 days, at which point cells were stimulated with 1 μM AP1510. After 24 h of stimulation, cells were fixed in 4% PFA, permeabilized in 0.2% Triton and incubated with the antibodies indicated for immunofluorescence. Images were all taken with preset exposure times. Cells that expressed HA at a level between 10 and 100 units of intensity according to ImageJ software were analysed for mislocalization of ZO-1.

Cell survival assay

MCF-10A cells expressing the mutants were plated at 0.6×10^6 cells per well of a six-well plate in growth media. Two days after plating, the media was replaced again with growth media +/− taxol in varying concentrations and ±1.0 μM AP1510. After 2 days in the presence or absence of drugs, the plates were washed three times in phosphate-buffered saline, fixed with a crystal violet solution (0.25% crystal violet in 20% methanol) for 10 min, washed six times in water and incubated in 700 μl lysis solution (51% water, 48% ethanol, 1% HCl) for

1 h. To quantitate the amount of crystal violet in each sample, 25 μl of the lysate was diluted in 975 μl of water, mixed and the optical density at 600 nm was determined using the spectrophotometer. Percent survival was calculated using the untreated condition as the denominator.

Antibodies

The HA antibody was obtained from Covance (Berkley, CA, USA), actin from Sigma, Ki67 from Zymed Laboratories (San Francisco, CA, USA) and NFGR from Chromoprobe (Maryland Heights, MO, USA). The Shc, phospho-tyrosine pY20 and Erk2 antibodies were all obtained from BD Transduction Laboratories (San Jose, CA, USA). Phospho-Ser 473-Akt, Akt, cleaved caspase-3 and phospho-p44/42MAPK were all from Cell Signaling (Danvers, MA, USA). Quantitation of blots was carried out with ImageJ (NIH) blot analysis.

Statistics

All statistics were performed using a standard Student's t-test.

Conflict of interest

The authors declare no conflict of interest.

References

Akiyama T, Matsuda S, Namba Y, Saito T, Toyoshima K, Yamamoto T. (1991). The transforming potential of the c-erbB-2 protein is regulated by its autophosphorylation at the carboxyl-terminal domain. *Mol Cell Biol* **11**: 833–842.

Aranda V, Haire T, Nolan ME, Calarco JP, Rosenberg AZ, Fawcett JP et al. (2006). Par6-aPKC uncouples ErbB2 induced disruption of polarized epithelial organization from proliferation control. *Nat Cell Biol* **8**: 1235–1245.

Buday L, Wunderlich L, Tamas P. (2002). The Nck family of adapter proteins: regulators of actin cytoskeleton. *Cell Signal* **14**: 723–731.

Coopman PJ, Do MT, Barth M, Bowden ET, Hayes AJ, Basyuk E et al. (2000). The Syk tyrosine kinase suppresses malignant growth of human breast cancer cells. *Nature* **406**: 742–747.

Dankort D, Jeyabalan N, Jones N, Dumont DJ, Muller WJ. (2001a). Multiple ErbB-2/Neu phosphorylation sites mediate transformation through distinct effector proteins. *J Biol Chem* **276**: 38921–38928.

Dankort D, Maslikowski B, Warner N, Kanno N, Kim H, Wang Z et al. (2001b). Grb2 and Shc adapter proteins play distinct roles in

Neu (ErbB-2)-induced mammary tumorigenesis: implications for human breast cancer. *Mol Cell Biol* **21**: 1540–1551.

Dankort DL, Muller WJ. (2000). Signal transduction in mammary tumorigenesis: a transgenic perspective. *Oncogene* **19**: 1038–1044.

Dankort DL, Wang Z, Blackmore V, Moran MF, Muller WJ. (1997). Distinct tyrosine autophosphorylation sites negatively and positively modulate neu-mediated transformation. *Mol Cell Biol* **17**: 5410–5425.

Debnath J, Mills KR, Collins NL, Reginato MJ, Muthuswamy SK, Brugge JS. (2002). The role of apoptosis in creating and maintaining luminal space within normal and oncogene-expressing mammary acini. *Cell* **111**: 29–40.

Feller SM. (2001). Crk family adaptors-signalling complex formation and biological roles. *Oncogene* **20**: 6348–6371.

Gu J, Tamura M, Pankov R, Danen EH, Takino T, Matsumoto K et al. (1999). Shc and FAK differentially regulate cell motility and directionality modulated by PTEN. *J Cell Biol* **146**: 389–403.

Habib T, Hejna JA, Moses RE, Decker SJ. (1998). Growth factors and insulin stimulate tyrosine phosphorylation of the 51C/SHIP2 protein. *J Biol Chem* **273**: 18605–18609.

Harrison SC. (1996). Peptide-surface association: the case of PDZ and PTB domains. *Cell* **86**: 341–343.

Henson ES, Hu X, Gibson SB. (2006). Herceptin sensitizes ErbB2-overexpressing cells to apoptosis by reducing antiapoptotic Mcl-1 expression. *Clin Cancer Res* **12**: 845–853.

Janes PW, Daly RJ, deFazio A, Sutherland RL. (1994). Activation of the Ras signalling pathway in human breast cancer cells over-expressing erbB-2. *Oncogene* **9**: 3601–3608.

Jones RB, Gordus A, Krall JA, MacBeath G. (2006). A quantitative protein interaction network for the ErbB receptors using protein microarrays. *Nature* **439**: 168–174.

Kim H, Chan R, Dankort DL, Zuo D, Najoukas M, Park M *et al.* (2005). The c-Src tyrosine kinase associates with the catalytic domain of ErbB-2: implications for ErbB-2 mediated signaling and transformation. *Oncogene* **24**: 7599–7607.

Knuefermann C, Lu Y, Liu B, Jin W, Liang K, Wu L *et al.* (2003). HER2/PI-3K/Akt activation leads to a multidrug resistance in human breast adenocarcinoma cells. *Oncogene* **22**: 3205–3212.

Leung WH, Bolland S. (2007). The inositol 5′-phosphatase SHIP-2 negatively regulates IgE-induced mast cell degranulation and cytokine production. *J Immunol* **179**: 95–102.

Marone R, Hess D, Dankort D, Muller WJ, Hynes NE, Badache A. (2004). Memo mediates ErbB2-driven cell motility. *Nat Cell Biol* **6**: 515–522.

Muthuswamy SK, Gilman M, Brugge JS. (1999). Controlled dimerization of ErbB receptors provides evidence for differential signaling by homo- and heterodimers. *Mol Cell Biol* **19**: 6845–6857.

Muthuswamy SK, Li D, Lelievre S, Bissell MJ, Brugge JS. (2001). ErbB2, but not ErbB1, reinitiates proliferation and induces luminal repopulation in epithelial acini. *Nat Cell Biol* **3**: 785–792.

Nahta R, Esteva FJ. (2007). Trastuzumab: triumphs and tribulations. *Oncogene* **26**: 3637–3643.

Nelson JM, Fry DW. (2001). Akt, MAPK (Erk1/2), and p38 act in concert to promote apoptosis in response to ErbB receptor family inhibition. *J Biol Chem* **276**: 14842–14847.

Orr GA, Verdier-Pinard P, McDaid H, Horwitz SB. (2003). Mechanisms of Taxol resistance related to microtubules. *Oncogene* **22**: 7280–7295.

Pupa SM, Tagliabue E, Menard S, Anichini A. (2005). HER-2: a biomarker at the crossroads of breast cancer immunotherapy and molecular medicine. *J Cell Physiol* **205**: 10–18.

Romond EH, Perez EA, Bryant J, Suman VJ, Geyer Jr CE, Davidson NE *et al.* (2005). Trastuzumab plus adjuvant chemotherapy for operable HER2-positive breast cancer. *N Engl J Med* **353**: 1673–1684.

Saucier C, Khoury H, Lai KM, Peschard P, Dankort D, Naujokas MA *et al.* (2004). The Shc adaptor protein is critical for VEGF induction by Met/HGF and ErbB2 receptors and for early onset of tumor angiogenesis. *Proc Natl Acad Sci USA* **101**: 2345–2350.

Slamon DJ, Clark GM, Wong SG, Levin WJ, Ullrich A, McGuire WL. (1987). Human breast cancer: correlation of relapse and survival with amplification of the HER-2/neu oncogene. *Science* **235**: 177–182.

Slamon DJ, Godolphin W, Jones LA, Holt JA, Wong SG, Keith DE *et al.* (1989). Studies of the HER-2/neu proto-oncogene in human breast and ovarian cancer. *Science* **244**: 707–712.

Slamon DJ, Leyland-Jones B, Shak S, Fuchs H, Paton V, Bajamonde A *et al.* (2001). Use of chemotherapy plus a monoclonal antibody against HER2 for metastatic breast cancer that overexpresses HER2. *N Engl J Med* **344**: 783–792.

Thomas D, Patterson SD, Bradshaw RA. (1995). Src homologous and collagen (Shc) protein binds to F-actin and translocates to the cytoskeleton upon nerve growth factor stimulation in PC12 cells. *J Biol Chem* **270**: 28924–28931.

Ursini-Siegel J, Hardy WR, Zuo D, Lam SH, Sanguin-Gendreau V, Cardiff RD *et al.* (2008). ShcA signalling is essential for tumour progression in mouse models of human breast cancer. *EMBO J* **27**: 910–920.

Verrills NM, Po'uha ST, Liu ML, Liaw TY, Larsen MR, Ivery MT *et al.* (2006). Alterations in gamma-actin and tubulin-targeted drug resistance in childhood leukemia. *J Natl Cancer Inst* **98**: 1363–1374.

Wada T, Penninger JM. (2004). Mitogen-activated protein kinases in apoptosis regulation. *Oncogene* **23**: 2838–2849.

Yarden Y, Sliwkowski MX. (2001). Untangling the ErbB signalling network. *Nat Rev Mol Cell Biol* **2**: 127–137.

Yu D, Jing T, Liu B, Yao J, Tan M, McDonnell TJ *et al.* (1998). Overexpression of ErbB2 blocks Taxol-induced apoptosis by upregulation of p21Cip1, which inhibits p34Cdc2 kinase. *Mol Cell* **2**: 581–591.

Zhan L, Xiang B, Muthuswamy SK. (2006). Controlled activation of ErbB1/ErbB2 heterodimers promote invasion of three-dimensional organized epithelia in an ErbB1-dependent manner: implications for progression of ErbB2-overexpressing tumors. *Cancer Res* **66**: 5201–5208.

Zhou BP, Hu MC, Miller SA, Yu Z, Xia W, Lin SY *et al.* (2000). HER-2/neu blocks tumor necrosis factor-induced apoptosis via the Akt/NF-kappaB pathway. *J Biol Chem* **275**: 8027–8031.

Supplementary Information accompanies the paper on the Oncogene website (http://www.nature.com/onc)